arXiv:hep-ph/9605356v1 20 May 1996

DESY 96-085
ANL-HEP-PR-96-39
hep-ph/9605356

Azimuthal Distribution of Quark-Antiquark Jets in DIS Diffractive Dissociation

J. Bartels[a], C. Ewerz[a], H. Lotter[a], M. Wüsthoff[b]

[a]II. Institut für Theoretische Physik,
Universität Hamburg, Germany[1]
[b]High Energy Physics Division,
Argonne National Laboratory, USA[2]

Abstract

We investigate the azimuthal distribution of quark-antiquark jets in DIS diffractive dissociation with large transverse momentum. In this kinematical region the matrix element is expressed in terms of the gluon structure function. For the transverse part of the cross section we find a $\cos(2\phi)$-distribution with the maximum at $\phi = \pm\pi/2$, i.e. the jets prefer a direction perpendicular to the electron plane. This is in contrast to boson gluon fusion where the $q\bar{q}$ jet cross section for transversely polarized bosons peaks at $\phi = 0$ and $\phi = \pi$. We discuss the origin of this striking difference and present numerical results relevant for the diffractive dissociation at HERA.

1.) The observation and analysis of diffractive events in deep inelastic electron proton scattering at HERA [1, 2, 3, 4] has attracted much attention recently. Particular interest has been given to the question whether this process is dominated by the same (soft) Pomeron which is observed in diffractive dissociation of hadron-hadron scattering, or by the hard Pomeron which is associated with the observed rise of F_2 at small x. As far as the (inclusive) diffractive structure function is concerned, one expects to see a combination of both the soft and the hard Pomeron. As a method of separating the hard component it has recently been suggested to look for final states of the diffractive system which consist of jets with large transverse momenta. The simplest configuration is a two-jet final state of a quark-antiquark pair. The cross section for this process, together with a

[1]Supported by Bundesministerium für Forschung und Technologie, Bonn, Germany under Contract 05 6HH93P(5) and EEC Program "Human Capital and Mobility" through Network "Physics at High Energy Colliders" under Contract CHRX-CT93-0357 (DG12 COMA).
[2]Supported by the US Department of Energy, High Energy Physics Division, Contract W-31-109-ENG-38.

few numerical predictions, has been presented in [5]. In this letter we continue this analysis by calculating, in the $\gamma^* -$ Pomeron center of mass system, the azimuthal distribution of the jets relative to the plane formed by the beam axis and the scattered electron. As we will show, this distribution differs from that of the photon-gluon fusion process and therefore presents a characteristic signal of the two gluon model for the hard Pomeron.

2.) The process that we are going to investigate is shown in Fig. 1a, and the variables are illustrated in Fig. 1b; for simplicity we restrict ourselves to the forward direction $t = 0$. Throughout this paper we work in the Pomeron-photon center of mass system. We begin with the subprocess $\gamma^* + \text{proton} \to q\bar{q} + \text{proton}$, and we take the incoming photon to be linearly polarized in the transverse direction. The polarization vectors are $e_x = (0, 1, 0, 0)$ and $e_y = (0, 0, 1, 0)$, and the electron momenta lie in the x-direction. We work in the leading-log $(1/x)$ approximation and use the **k**-factorization theorem [6] to express the amplitude through the unintegrated gluon distribution of the proton. This is based on the assumption that the total energy $s = (q + p)^2$ is much larger than the photon virtuality $Q^2 = -q^2$ and the invariant mass of the outgoing quark anti-quark pair $M^2 = (q + x_{I\!P} p)^2$. The quark phase space is parameterized in terms of the quarks transverse momentum $k_\perp = |k_\perp|(e_x \cos\phi + e_y \sin\phi)$, and its longitudinal momentum fraction α according to the Sudakov decomposition $k_\mu = \alpha q'_\mu + \mathbf{k}^2/(2\alpha pq')p_\mu + k_{\perp\mu}$ with $q' = q + xp$ and $\mathbf{k}^2 = -k_{\perp\mu}k^\mu_\perp$. The invariant mass M^2 is related to the transverse momentum through $\mathbf{k}^2 = \alpha(1-\alpha)M^2$. The differential cross section for the incoming photon with a polarization lying in the electron plane has the form:

$$\frac{d^{\gamma^* p}_{D,T}}{dM^2 d\mathbf{k}^2 dt d\phi}_{|t=0} = \frac{d^{\gamma^* p}_{D,T}}{dM^2 d\mathbf{k}^2 dt}_{|t=0} - 2\frac{\frac{\mathbf{k}^2}{M^2}}{1 - 2\frac{\mathbf{k}^2}{M^2}} \cos 2\phi \frac{d^{\gamma^* p}_{D,T}}{dM^2 d\mathbf{k}^2 dt}_{|t=0} \tag{1}$$

where $\frac{d\sigma^{\gamma^* p}_{D,T}}{dM^2 d\mathbf{k}^2 dt}$ will be given below in eq. (8). The main feature to be noticed is the minus sign in front of the angular dependent piece of the cross section. It is opposite to the sign structure of the photon-gluon fusion process [7] (which will be discussecd below), and it leads to a characteristic maximum of the cross section[3] at $\phi = \pi/2$. For the incoming photon being polarized in the y-direction the cross section has the same form as (1), but with a plus sign in front of the second term.

Turning to electroproduction, we have to sum over all polarizations of the virtual photon; the interference of longitudinal and transverse polarizations leads to an additional azimuthal dependence. We need the Sudakov parametrization of the electron momentum:

$$\ell_\mu = \frac{1}{y} q'_\mu + (1-y)\frac{x}{y} p_\mu + \ell_{\perp\mu} \;\;,\;\; \ell^2_\perp = -\frac{1-y}{y^2} Q^2 \;\;,\;\; \ell_\perp = |\ell_\perp| e_x \tag{2}$$

Inserting this into the usual lepton tensor:

$$L_{\mu\nu} = 2\left[\ell_\mu \ell_\nu - \frac{Q^2}{4} g_{\mu\nu}\right] \tag{3}$$

[3] A similar phenomenon has been observed in the azimuthal distribution of forward jets in deep inelastic electron proton scattering [8, 9].

and contracting with the photon polarization vectors we arrive at the following flux factors for the linearly polarized transverse photons

$$L_{\mu\nu}e_x^\mu e_x^\nu = \frac{1}{2}\,Q^2 + 2\frac{1-y}{y^2}\,Q^2 \tag{4}$$

$$L_{\mu\nu}e_y^\mu e_y^\nu = \frac{1}{2}\,Q^2 \tag{5}$$

Summing over all polarizations we arrive at the ep-cross section:

$$\frac{d\sigma_D^{e^-p}}{dydQ^2dM^2d\mathbf{k}^2d\phi dt}_{|t=0} = \frac{\alpha_{em}}{yQ^2\pi}\left[\frac{1+(1-y)^2}{2}\frac{d\sigma_{D,T}^{\gamma^*p}}{dM^2d\mathbf{k}^2dt}_{|t=0} - 2(1-y)\frac{\frac{\mathbf{k}^2}{M^2}}{1-2\frac{\mathbf{k}^2}{M^2}}\cos 2\phi\frac{d\sigma_{D,T}^{\gamma^*p}}{dM^2d\mathbf{k}^2dt}_{|t=0}\right.$$
$$\left. +(1-y)\frac{d\sigma_{D,L}^{\gamma^*p}}{dM^2d\mathbf{k}^2dt}_{|t=0} + (2-y)\sqrt{1-y}\cos\phi\frac{d\sigma_{D,I}^{\gamma^*p}}{dM^2d\mathbf{k}^2dt}_{|t=0}\right] \tag{6}$$

where the indices T, L, and I refer to the contributions of transverse and longitudinal photons and the interference term, resp. Apart from the flux factors of the photons, the transverse part has the same structure as seen in eq. (1). In particular, the minus sign in front of the angular dependent term is a direct consequence of combining (1) with the flux factor in (4).

Eq.(6) is written for the case in which the polar-angle θ ($\cos\theta = 1-2\alpha$), the angle between the quark jet with momentum k and the proton (Pomeron), is restricted to be smaller than $\pi/2$, i.e. α varies between 0 and 1/2. If this jet lies in the other hemisphere (polar angle θ between $\pi/2$ and π or, equivalently, α between 1/2 and 1), the last term in (6) changes sign. When averaging over both hemispheres the cross section above has to be multiplied with a factor of two, and the interference term disappears. Then, the only angular dependence results from the term proportional to $\cos 2\phi$ in eq. (6). Note the additional factor $\mathbf{k}^2$ in front of this term. We therefore expect the azimuthal asymmetry to be more pronounced at large transverse momenta (at the same time, however, the cross section decreases with growing transverse momentum). Finally, by integrating the cross section from 0 to 2π we recover our previous result [5]. A numerical analysis of the above formulae will be performed in part **4.)**.

The expressions for the longitudinal and transverse photon-proton cross sections have been obtained in [5]:

$$2\pi\frac{d\sigma_{D,L}^{\gamma^*p}}{dM^2d\mathbf{k}^2dt}_{|t=0} = \frac{1}{M^4}\frac{\mathbf{k}^2}{Q^2}\frac{1}{\sqrt{1-4\frac{\mathbf{k}^2}{M^2}}}\frac{2}{3}\sum_f e_f^2\alpha_{em}\pi^2\alpha_s^2\left[I_L(Q^2,M^2,\mathbf{k}^2)\right]^2 \tag{7}$$

$$2\pi\frac{d\sigma_{D,T}^{\gamma^*p}}{dM^2d\mathbf{k}^2dt}_{|t=0} = \frac{1}{M^4}\frac{1-2\frac{\mathbf{k}^2}{M^2}}{\sqrt{1-4\frac{\mathbf{k}^2}{M^2}}}\frac{1}{24}\sum_f e_f^2\alpha_{em}\pi^2\alpha_s^2\left[I_T(Q^2,M^2,\mathbf{k}^2)\right]^2 \tag{8}$$

In the same spirit we find for the interference contribution

$$2\pi\frac{d\sigma_{D,I}^{\gamma^*p}}{dM^2d\mathbf{k}^2dt}_{|t=0} = \frac{1}{M^4}\left(\frac{\mathbf{k}^2}{Q^2}\right)^{\frac{1}{2}}\frac{1}{6}\sum_f e_f^2\alpha_{em}\pi^2\alpha_s^2 I_T(Q^2,M^2,\mathbf{k}^2)I_L(Q^2,M^2,\mathbf{k}^2) \tag{9}$$

with

$$I_T = -\int \frac{d\mathbf{l}^2}{\mathbf{l}^2}\left[\frac{M^2-Q^2}{M^2+Q^2}+\frac{\mathbf{l}^2+\frac{\mathbf{k}^2}{M^2}(Q^2-M^2)}{\sqrt{(\mathbf{l}^2+\frac{\mathbf{k}^2}{M^2}(Q^2-M^2))^2+4\mathbf{k}^4\frac{Q^2}{M^2}}}\right]\mathcal{F}_G(x_{I\!P},\mathbf{l}^2) \tag{10}$$

$$I_L = -\int \frac{d\mathbf{l}^2}{\mathbf{l}^2}\left[\frac{Q^2}{M^2+Q^2}-\frac{\mathbf{k}^2Q^2}{M^2\sqrt{(\mathbf{l}^2+\frac{\mathbf{k}^2}{M^2}(Q^2-M^2))^2+4\mathbf{k}^4\frac{Q^2}{M^2}}}\right]\mathcal{F}_G(x_{I\!P},\mathbf{l}^2) \tag{11}$$

and the unintegrated gluon distribution of the proton

$$\int^{Q^2} d\mathbf{l}^2\mathcal{F}_G(x_{I\!P},\mathbf{l}^2) = x_{I\!P}G(x_{I\!P},Q^2) \tag{12}$$

In our expression (12) we have used, for the two-gluon subamplitude, the (forward) gluon structure function of the proton. Strictly speaking, this is not quite accurate, because the longitudinal momenta of the two gluon lines differ by $x_{I\!P}p$. In our leading-log calculation, however, we cannot distinguish between this 'slightly nonforward' gluon structure function and the usual DIS gluon structure function. We therefore shall use the usual gluon density of the proton, and, as a consequence, we have to accept an error in the absolute normalization which is characteristic for a leading-log calculation (cf. the discussion in [5]).

Without going into more detail we quote the results that were obtained in [5] for the functions I_T, I_L above

$$I_T = \left[\frac{4Q^2M^4}{\mathbf{k}^2(M^2+Q^2)^3}+b_T\frac{\partial}{\partial\mathbf{k}^2}\right]x_{I\!P}G(x_{I\!P},\mathbf{k}^2\frac{Q^2+M^2}{M^2}) \tag{13}$$

$$I_L = \left[\frac{Q^2M^2(Q^2-M^2)}{\mathbf{k}^2(M^2+Q^2)^3}+b_L\frac{\partial}{\partial\mathbf{k}^2}\right]x_{I\!P}G(x_{I\!P},\mathbf{k}^2\frac{Q^2+M^2}{M^2}) \tag{14}$$

In these expressions the first terms represent the double leading log approximation. As discussed in [5], the derivative terms with the functions b_T, b_L of Q^2 and M^2 are those next-to-leading order (in $\log\mathbf{k}^2(M^2+Q^2)/M^2$) corrections which, as we believe, are numerically most important. They can be found in eqs. (12), (13) of [5] and will not be given explicitly here. We wish, however, to stress that these next-to-leading order corrections are not complete, and we believe that a systematic study of order-α_s corrections to our 'Born approximation' remains an important future task.

3.) It will be useful to compare our results with the usual photon gluon fusion cross section. To be definite, let us, again, consider the cross section for the production of a quark-antiquark pair in the kinematic region where W^2 is much larger than Q^2. The momenta are labelled as shown in Fig. 2. The gluon momentum l_μ has the Sudakov decomposition $l=\eta p+l_\perp$ with $\eta = x_B(1+W^2/Q^2)$ (the component along the momentum q' is small and can be neglected), and the polarization vector of the gluon is $p_\mu\sqrt{2/W^2}$. Choosing the incoming photon to have the transverse polarization in the x-direction, and summing over the quark helicities, we obtain for the square of the subprocess $\gamma^*+g\to q\bar{q}$:

$$\mathbf{e}_x\cdot\mathbf{e}_x\ \mathbf{V}\cdot\mathbf{V}-\ 4\alpha(1-\alpha)\mathbf{e}_x\cdot\mathbf{V}\ \ \mathbf{e}_x\cdot\mathbf{V} \tag{15}$$

where we have disregarded overall constants, and the vector $\mathbf{V}$ is defined as

$$\mathbf{V} = \frac{\mathbf{k}}{D(\mathbf{k})} - \frac{\mathbf{k}-\mathbf{l}}{D(\mathbf{k}-\mathbf{l})} \ , \ D(\mathbf{k}) = \alpha(1-\alpha)Q^2 + \mathbf{k}^2 \tag{16}$$

As can be seen from (16), the vector $\mathbf{V}$ can be interpreted as the $q\bar{q}$ component of the wave function of the transverse photon. It has the form of a dipole. The standard result for the photon-gluon fusion process is obtained by integrating over the azimuthal angle ϕ_l of the gluon and taking the limit $\mathbf{l}^2 \to 0$. For small $\mathbf{l}^2$ one finds

$$\int \frac{d\phi_l}{2\pi} \mathbf{V}_i \mathbf{V}_j = \frac{\mathbf{l}^2}{2D(\mathbf{k})^2} \left(\delta_{ij} - \mathbf{k}_i \mathbf{k}_j \frac{\mathbf{k}^2 Q^2}{M^2 [D(\mathbf{k})]^2} \right) \tag{17}$$

and the cross section becomes

$$d\sigma \sim \left(1 - 2\frac{\mathbf{k}^2}{M^2} \right) \frac{Q^4 + M^4}{(Q^2+M^2)^2} + 4\frac{\mathbf{k}^2}{M^2} \cos 2\phi \frac{Q^2 M^2}{(Q^2+M^2)^2} \tag{18}$$

The angular part now has a positive sign, quite in contrast to the previous case ((1) or (6)). This difference can be traced back to the δ_{ij} piece in eq. (17): the second term $\sim \mathbf{k}_i \mathbf{k}_j$ alone would have lead to the same structure as (1), and it is the first term which leads to the sign change in (18). As an attempt to find a physical interpretation, one might interpret the contribution $\sim \mathbf{k}_i \mathbf{k}_j$ as an incoherent product of the two dipoles, whereas the term $\sim \delta_{ij}$ represents a correlation between the dipole and its conjugate which results from the angular integral.

For comparison we write down the analogue of eq. (15) for the diffractive case, i.e. the expression for the square of the subprocess $\gamma^* + 2g \to q\bar{q}$ (Fig. 1a). It has the same form as (15), but now we have two $\mathbf{l}$-integrals (both for the matrix element and its complex conjugate). The wave functions $\mathbf{V}$ in (15) have to be replaced by $\mathbf{V}_D(\mathbf{l})$ and $\mathbf{V}_D(\mathbf{l}')$:

$$\mathbf{e}_x \cdot \mathbf{e}_x \ \mathbf{V}_D(\mathbf{l}) \cdot \mathbf{V}_D(\mathbf{l}') - \ 4\alpha(1-\alpha)\, \mathbf{e}_x \cdot \mathbf{V}_D(\mathbf{l}) \ \ \mathbf{e}_x \cdot \mathbf{V}_D(\mathbf{l}') \tag{19}$$

where

$$\mathbf{V}_D(\mathbf{l}) = 2\frac{\mathbf{k}}{D(\mathbf{k})} - \frac{\mathbf{k}-\mathbf{l}}{D(\mathbf{k}-\mathbf{l})} - \frac{\mathbf{k}+\mathbf{l}}{D(\mathbf{k}+\mathbf{l})}. \tag{20}$$

The limit $\mathbf{l}^2 \to 0$ and the angular integration are done independently for both $\mathbf{l}$ and $\mathbf{l}'$. For the leading term in this limit we find

$$\int \frac{d\phi_l}{2\pi} \mathbf{V}_D(\mathbf{l}) = \mathbf{k} \frac{4\, Q^2 M^4}{(Q^2+M^2)^3} \frac{\mathbf{l}^2}{\mathbf{k}^4} \left[1 + O(\mathbf{l}^2) \right] \tag{21}$$

As a result, the tensor $\mathbf{V}_i \mathbf{V}_j$ is proportional to $\mathbf{k}_i \mathbf{k}_j$, and there is no contribution proportional to δ_{ij}.

To complete our review of the photon-gluon fusion process, we mention that - unlike in the usual discussion where only the leading term of the limit $\mathbf{l}^2 \to 0$ is retained - a consistent application of the $\mathbf{k}_T$-factorization allows to consider also the case $\mathbf{l}^2 \neq 0$. As one can see immediately from the kinematics in Fig. 2, in this case the momentum transfer from the proton system is no longer zero. When integrating over $\mathbf{l}$, one at the same time averages over the transverse momentum of one of

the two jets, and as a result the cross section can no longer be compared with the diffractive cross section of the first part. Nevertheless, we still can ask for the azimuthal dependence of the jet with fixed momentum $\mathbf{k}^2$. Having performed the ϕ_l integral, one arrives at a tensor structure similar to (17), but the coefficient functions of the two terms might be quite different. Consequently, also the sign structure in the cross section in (18), which results from a combination of these coefficient functions, may change, and the azimuthal dependence of the cross section will depend upon the $\mathbf{l}$-dependence of the gluon distribution. A definite prediction could be made if one uses the BFKL Pomeron as a model for the gluon structure function. In analogy with the results of [5] one expects, as a correction to the DLA result (18), a term containing the unintegrated gluon distribution. Details of such a calculation will be presented elsewhere [10].

4. In this section we want to present some numerical results based on the formula eq. (6). In our analysis we closely follow the strategy described in [5]. For the diffractive cross section the integration over t is performed after multiplication of our $t = 0$ expression with the Donnachie–Landshoff formfactor. We use the GRV next to leading order parameterization [11] of the gluon density and take account of the subleading corrections, indicated as b_T, b_L in eqs. (13), (14). For the nondiffractive case where we do not calculate corrections of this kind, we take the GRV leading order density. In both cases we take α_s running with the scale equal to the momentum scale of the gluon density.

First, to get an overall impression we show in Fig. 3, as a function of the azimuthal angle ϕ, the totally integrated electron proton cross section with the kinematical constraints $Q^2 > 10\,\mathrm{GeV}^2, x_{I\!P} < 10^{-2}, \mathbf{k}^2 > 2\,\mathrm{GeV}^2$ and $50\,\mathrm{GeV}^2 < W < 220\,\mathrm{GeV}^2$. Note that, for given values of M^2 and $\mathbf{k}^2$, we have summed over the two configurations with $\alpha = \frac{1}{2}+\frac{1}{2}\sqrt{1-4\mathbf{k}^2/M^2}$ and $\alpha = \frac{1}{2}-\frac{1}{2}\sqrt{1-4\mathbf{k}^2/M^2}$, i. e. over the two different hemispheres. In addition we added the degenerate contribution with $\phi + \pi$, i. e. the total cross section is recovered by integrating $d\sigma/d\phi$ from $\phi = 0$ up to $\phi = \pi$. As a result, the interfence term in (6) drops out, and our curves are symmetric w.r.t. $\phi = \pi/2$. For comparison we also show the contribution of the longitudinal polarization (dashed line) and the ϕ-independent part of the transverse polarization (dotted line). The angle dependent contribution leads to a factor of approximately 2 between the minimum of the cross section at $\phi = 0, \pi$ and the maximum at $\phi = \pi/2$. Furthermore, one notices that the longitudinal polarization gives on the whole a 10% contribution to the total cross section. As to the differential cross section, the relative magnitude of the maximum, as well as the contribution of the longitudinal polarization, will depend on the kinematic variables, especially $\beta = Q^2/(Q^2+M^2)$ (cf.the discussion in [5]).

Next we want to exhibit the influence of the kinematical prefactors on the relative magnitude of the azimuthally asymmetric contribution. In Fig. 4 we show again the totally integrated *ep* - cross section with the above given cuts for $Q^2, x_{I\!P}$ and W but with three different cuts in $\mathbf{k}^2$. The curves demonstrate that a restriction of the phase space to larger $\mathbf{k}^2$ leads to an increase of the asymmetry, due to an additional $\mathbf{k}^2$ in the prefactor of the angular dependent term. The absolute magnitude of the cross section, however, decreases due to the overall suppression at large transverse momenta.

Instead of $\mathbf{k}^2$, it might be more convenient to use the polar angle θ (Fig. 2) between the jet with momentum k and the Pomeron momentum in the photon-Pomeron cm-system. This angle is determined through $\sin^2\theta = 4\mathbf{k}^2/M^2$. Here we do not add the configuration at $\phi + \pi$. The cross

section for $\phi > \pi$ is obtained by reflection w.r.t. the axis $\phi = \pi$. To make sure that we do not get a contribution from a region where our perturbative analysis is not reliable we have imposed an absolute lower cutoff on $\mathbf{k}^2$ of $1\,\mathrm{GeV}^2$. In addition we have chosen bins in M^2 to keep the center of mass energy of the photon-pomeron subprocess roughly constant. In Fig. 5 we present the cross section with cuts in θ instead of cuts in $\mathbf{k}^2$ imposed. Now the interference term in (6) can no longer be neglected, and we expect a slight asymmetry between $\phi = 0$ and $\phi = \pi$. In the left diagram we have chosen $20\,\mathrm{GeV}^2 < M^2 < 50\,\mathrm{GeV}^2$ and two different cuts in θ, $\pi/16 < \theta < \pi/4$ (upper curve) and $\pi/4 < \theta < \pi/2$ (lower curve), respectively. Again, as expected, for larger θ, corresponding to larger $\mathbf{k}^2$, the asymmetry is more pronounced, but the normalization is smaller. The $\cos\phi$-asymmetry is clearly visible and it can be seen that the coefficent of the $\cos\phi$-term is positive. In the right diagramm we have chosen the same θ-cuts but the M^2-bin $50\,\mathrm{GeV}^2 < M^2 < 100\,\mathrm{GeV}^2$. Here the coefficent of the $\cos\phi$-term is negative. This is due to the fact that for large masses the function I_L (eq. (14)) becomes negative. This sign change is a unique property of the interference term.

Finally we want to illustrate the essential difference between the diffractive cross section based on the two gluon exchange model and the boson gluon fusion cross section. We have calculated the total cross section for quark-antiquark jet production in *ep*-scattering based on the photon gluon fusion mechanism. The explicit formulae for this cross section can be obtained with the method sketched in **3.)** and can be found in [7]. In Fig. 6 we present the normalized (to unit integral) differential cross section in ϕ with all other variables integrated using the cuts $Q^2 > 10\,\mathrm{GeV}^2, \eta < 10^{-2}, \mathbf{k}^2 > 2\,\mathrm{GeV}^2$ and $50\,\mathrm{GeV}^2 < W^2 < 220\,\mathrm{GeV}^2$. This curve nicely demonstrates that in the boson gluon fusion case the jets prefer a direction in the electron plane (defined by $\phi = 0$), whereas in the two gluon exchange case (Figs. 3-5) the jets prefer a perpendicular direction.

5.) In this paper we have calculated the azimuthal dependence of two quark-antiquark jets with large transverse momenta in DIS diffractive dissociation. Our main result, contained in eq. (6), is the striking sign structure of the angle dependent term. It leads to a characteristic maximum of the cross section at $\phi = \pi/2$, quite in contrast to the angular dependence of the photon-gluon fusion subprocess which peaks at 0 and π. An experimental observation of this maximum at $\pi/2$ would clearly confirm our present understanding of the 'hard Pomeron'.

Some time ago it has been suggested that the photon-gluon fusion subprocess, accompanied by the additional exchange of soft gluons [12] or by a suitable modification of the final state interactions [13] might represent the basic mechanism of the diffractive dissociation observed at HERA. In principle, the different dependencies upon ϕ discussed in this letter might help to discriminate between the two mechanisms: the exchange of a color singlet two-gluon state (hard Pomeron) and the single gluon exchange in the photon-gluon fusion model. There are, however, two *caveats* to be kept in mind. First, the perturbative calculation of the two-gluon exchange can be justified only for jets with large transverse momenta; this excludes any prediction for the diffractive structure function which may very well be dominated by soft final states (e.g. Pomeron-remnant jets). The discussion in [12], on the other hand, refers to the diffractive structure function and not to specific final states. Secondly, for the case of the photon-gluon fusion we do not know to what extent final state hadronization will modify the azimuthal dependence of the partonic cross section: since the $q\bar{q}$ pair is in a color octet state, one expects a color connection with the proton system which may affect the angular distribution. In contrast, for the two-gluon exchange model we believe that the partonic cross section is rather robust against hadronization effects. Namely, our perturbative cal-

culation describes the azimuthal distribution of the $q\bar{q}$ dipole which initially has a small transverse size. The subsequent hadronization will be restricted to the $q\bar{q}$-system, and thereby not change the orientiation.

In summary, final states in the diffractive dissociation of the photon which contain only hard jets represent a novel class of hard processes which are calculable in perturbative QCD: jet production from the 'annihilation' of a photon and a color singlet two-gluon state (a hard Pomeron). The $q\bar{q}$ jets considered in [5] and in the present paper represent the very first step along this line – somewhat analogous to the two-jet final states in e^+e^- annihilation. What has to come next is the order-α_s correction to the two-jet configuration, together with the three-jet final state.

References

[1] H1 Collaboration, *Phys. Lett.* **B 348** (1995) 681.

[2] H1 Collaboration, presented at the DIS 96 conference in Rome (to appear in the proceedings).

[3] ZEUS Collaboration, *Z. Phys.* **C 68** (1995) 569.

[4] ZEUS Collaboration, *Z. Phys.* **C 70** (1996) 391.

[5] J.Bartels, H.Lotter, M.Wüsthoff, *Phys. Lett.* **B** (to appear).

[6] S.Catani, F.Hautmann, *Nucl. Phys.* **B 427** (1995) 475.

[7] H.Georgi, J.Sheiman, *Phys. Rev.* **D 20** (1979) 111;
Ch.Rumpf, G.Kramer, *Phys. Lett.* **B 89** (1980) 380;
Ch.Rumpf, G.Kramer, J.Willrodt, *Z. Phys.* **C 7** (1981) 337.

[8] J.Bartels, V.DelDuca, D.Graudenz, A.DeRoeck, M.Wüsthoff, DESY 96-036, hep-ph/9604272 (accepted for publication in *Phys. Lett.* **B**).

[9] J.Bartels, V.DelDuca, M.Wüsthoff, (in preparation).

[10] H.Lotter, in preparation.

[11] M.Glück, E.Reya, A.Vogt, *Z. Phys.* **C 67** (1995) 433.

[12] W.Buchmüller, A.Hebecker, *Phys. Lett.* **B 355** (1995) 573.

[13] A.Edin, G.Ingelman, J.Rathsman, *Phys. Lett.* **B 366** (1996) 371.

Figure Captions

Fig. 1a : One of the four diagrams contributing to the hard process $\gamma^* + p \to q\bar{q} + p$. The outgoing (anti)quark momenta are fixed and the same for all four diagrams. The blob depicts the unintegrated gluon structure function $\mathcal{F}_G$.

Fig. 1b : Definition of planes and angles in the $\gamma^* I\!P$ cms ($\vec{q} + x_{I\!P}\vec{p} = 0$). The leptonic plane is given by the vectors $\vec{\ell}$ and $\vec{q} = \vec{\ell} - \vec{\ell}'$, the jet plane by the vectors $x_{I\!P}\vec{p}$ and $\vec{k}$). ϕ is the angle between these two planes. θ is the polar angle of the jet direction $\vec{k}$.

Fig. 2 : One of the two diagrams for the boson gluon fusion (BGF) process. The square of the BGF amplitude again leads to the gluon structure function.

Fig. 3 : The ϕ dependence of the ep - cross section in eq. (6) integrated over the other variables. Displayed is the sum of all terms (solid line), and the contribution of the angular independent transverse (dotted line) and longitudinal (dashed line) terms.

Fig. 4 : The ϕ dependence of total ep - cross section with different cuts in $\mathbf{k}^2$: $1\,\mathrm{GeV}^2 < \mathbf{k}^2 < 2\,\mathrm{GeV}^2$, $2\,\mathrm{GeV}^2 < \mathbf{k}^2$, $5\,\mathrm{GeV}^2 < \mathbf{k}^2$ (from top to bottom).

Fig. 5 : The ϕ dependence of total ep - cross section with different cuts in θ and M^2. In the left diagram we have $20\,\mathrm{GeV}^2 < M^2 < 50\,\mathrm{GeV}^2$ and $\pi/16 < \theta < \pi/4$ (upper curve), $\pi/4 < \theta < \pi/2$ (lower curve). In the right diagram we have $50\,\mathrm{GeV}^2 < M^2 < 100\,\mathrm{GeV}^2$ and $\pi/16 < \theta < \pi/4$ (upper curve), $\pi/4 < \theta < \pi/2$ (lower curve).

Fig. 6 : Normalized differential cross section for two jet production based on the boson-gluon fusion mechanism.

Figures

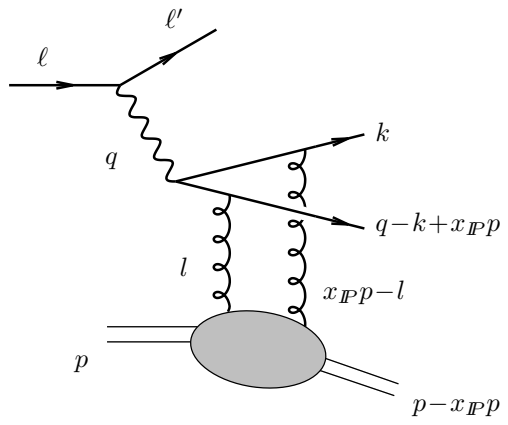


Figure 1a:

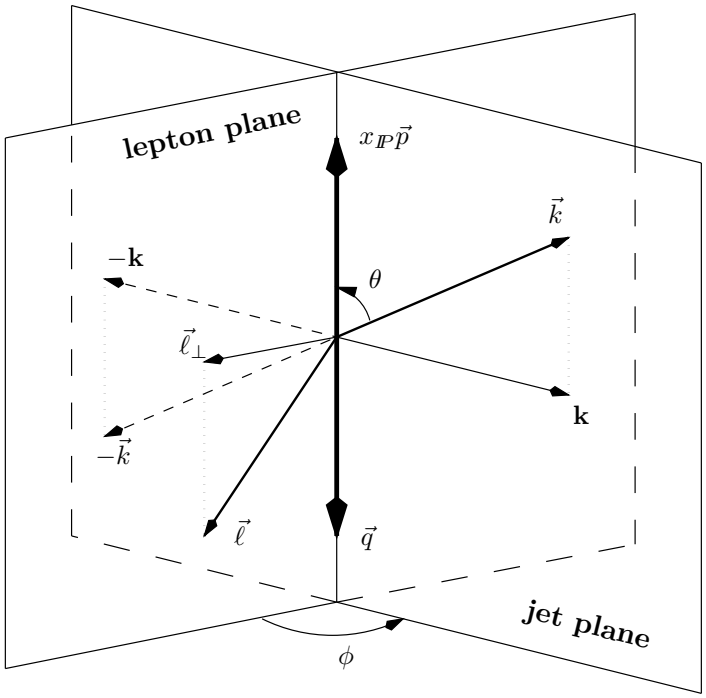


Figure 1b:

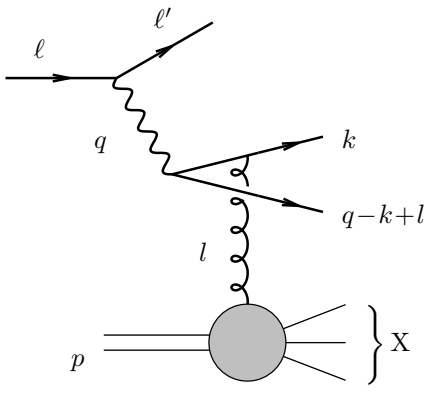


Figure 2:

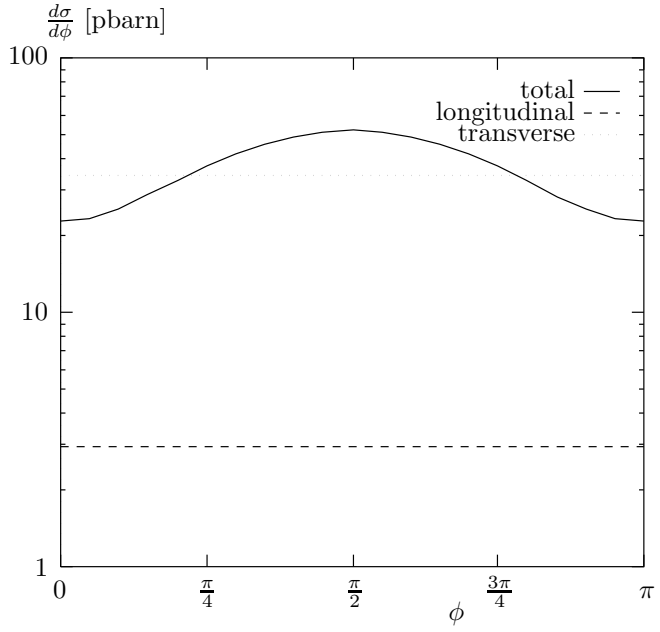


Figure 3:

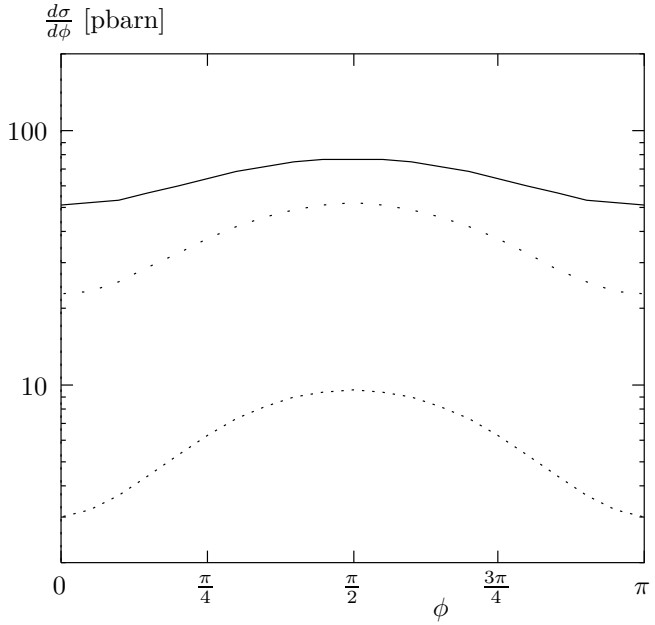


Figure 4:

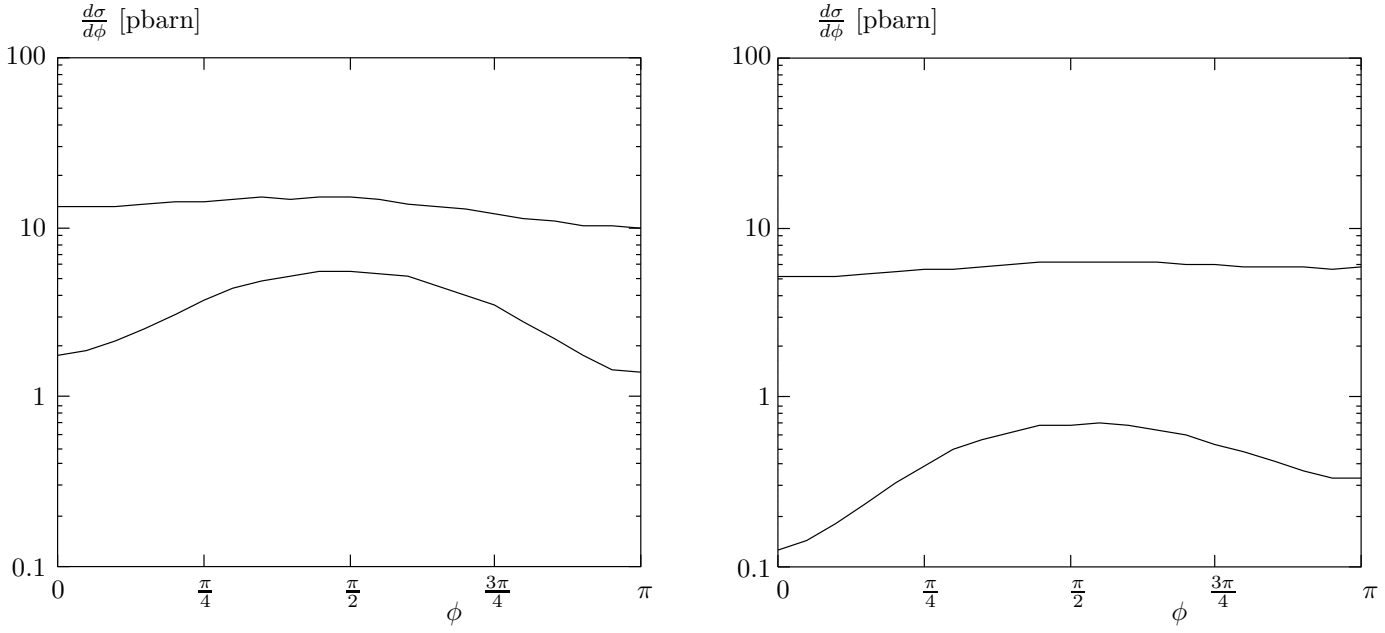


Figure 5:

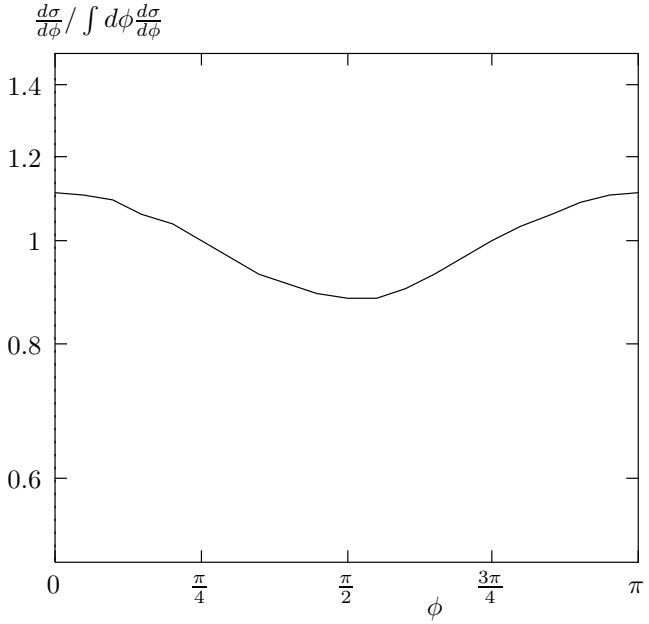


Figure 6: